CNGC2 Is a Ca^{2+} Influx Channel That Prevents Accumulation of Apoplastic Ca^{2+} in the Leaf[1]

Yan Wang[2], Yan Kang[2], Chunli Ma[2], Ruiying Miao, Caili Wu, Yu Long, Ting Ge, Zinian Wu, Xiangyang Hou, Junxia Zhang, and Zhi Qi*

Inner Mongolia University, School of Life Sciences, Hohhot 010021, People's Republic of China (Y.W., Y.K., C.M., R.M., C.W., Y.L., T.G., J.Z., Z.Q.); and Institute of Grassland Research, Chinese Academy of Agricultural Sciences, Hohhot 010010, People's Republic of China (Z.W., X.H.)

ORCID ID: 0000-0002-0224-5701 (Z.Q.).

Ca^{2+} is absorbed by roots and transported upward through the xylem to the apoplastic space of the leaf, after which it is deposited into the leaf cell. In Arabidopsis (*Arabidopsis thaliana*), the tonoplast-localized Ca^{2+}/H^+ transporters CATION EXCHANGER1 (CAX1) and CAX3 sequester Ca^{2+} from the cytosol into the vacuole, but it is not known what transporter mediates the initial Ca^{2+} influx from the apoplast to the cytosol. Here, we report that Arabidopsis *CYCLIC NUCLEOTIDE-GATED CHANNEL2* (*CNGC2*) encodes a protein with Ca^{2+} influx channel activity and is expressed in the leaf areas surrounding the free endings of minor veins, which is the primary site for Ca^{2+} unloading from the vasculature and influx into leaf cells. Under hydroponic growth conditions, with 0.1 mM Ca^{2+}, both Arabidopsis *cngc2* and *cax1cax3* loss-of-function mutants grew normally. Increasing the Ca^{2+} concentration to 10 mM induced H_2O_2 accumulation, cell death, and leaf senescence and partially suppressed the hypersensitive response to avirulent pathogens in the mutants but not in the wild type. In vivo apoplastic Ca^{2+} overaccumulation was found in the leaves of *cngc2* and *cax1cax*3 but not the wild type under the 10 mM Ca^{2+} condition, as monitored by Oregon Green BAPTA 488 5N, a low-affinity and membrane-impermeable Ca^{2+} probe. Our results indicate that CNGC2 likely has no direct roles in leaf development or the hypersensitive response but, instead, that CNGC2 could mediate Ca^{2+} influx into leaf cells. Finally, the in vivo extracellular Ca^{2+} imaging method developed in this study provides a new tool for investigating Ca^{2+} dynamics in plant cells.

Deciphering the molecular mechanisms underlying plant mineral nutrition will provide a foundation for improving the productivity of modern crops and forests (Karley and White, 2009; Liu et al., 2015; Pilbeam, 2015). Although significant progress has been made in elucidating the cellular and genetic pathways of nitrogen, phosphorus, and potassium uptake and distribution in plants in the past decade (Baker et al., 2015; Krapp, 2015; Wang and Wu, 2015), the corresponding pathways remain largely unknown for Ca (Gilliham et al., 2011; Kumar et al., 2015), an essential mineral that stabilizes cellular structures and acts as an important intracellular messenger (Dodd et al., 2010; Kudla et al., 2010; Reddy et al., 2011; Spalding and Harper, 2011; Yang et al., 2012). Ecological evidence indicates that Ca concentrations have decreased in forest soils and fresh water worldwide over the past century (Johnson et al., 2008; Bedison and Johnson, 2010; Talhelm et al., 2012; Leys et al., 2016). This Ca decrease has increased the susceptibility of forest and crop plants to stressful conditions (Hong-Bo et al., 2008; Genc et al., 2010; Halman et al., 2011) and reduced the diversity of plant species (Närhi et al., 2011). Understanding the genetic mechanisms by which Ca is absorbed by the roots and distributed in the leaves is important for addressing this environmental challenge and for breeding crops with better Ca nutrition (Robertson, 2013).

Ca^{2+} is absorbed by root cells, uploaded into the xylem, and further transported to the aerial parts of the plant, where it is unloaded from the xylem and redistributed into all types of leaf cells (White, 2001; White and Broadley, 2003; Gilliham et al., 2011). Whereas Ca^{2+} absorption and distribution have been studied at the physiological level (Kumar et al., 2015), the underlying molecular

[1] This work was supported by the National Natural Science Foundation of China (grant nos. 31571448 and 31171364 to Z.Q.), by the Collaborative Innovation Center of Grassland, Ecology, and Husbandry, Department of Education of Inner Mongolia Autonomous Region, People's Republic of China (to Z.Q.), and by the Agricultural Science and Technology Innovation Program of the Chinese Academy of Agricultural Sciences (grant no. CAAS-ASTIP-2016-IGRCAAS to Z.W. and X.H.).

[2] These authors contributed equally to the article.

* Address correspondence to qizhi@imu.edu.cn.

The author responsible for distribution of materials integral to the findings presented in this article in accordance with the policy described in the Instructions for Authors (www.plantphysiol.org) is: Zhi Qi (qizhi@imu.edu.cn).

Z.Q. and Y.K. designed experiments; Y.W., Y.K., and C.M. performed most experiments; R.M. carried out hydroponics-based phenotype analysis; Y.L. performed the patch-clamp experiment; T.G., J.Z., and C.W. carried out homozygous mutant identification and performed the initial phenotype study; Z.W. and X.H. did the mineral elements measurement; Y.W., Y.K., C.M., and Z.Q analyzed data; Z.Q., Y.W., and Y.K. wrote the article.

www.plantphysiol.org/cgi/doi/10.1104/pp.16.01222

mechanisms remain largely unknown (Kudla et al., 2010; Spalding and Harper, 2011). Suberin deposits in the roots form a barrier that limits the accumulation of mineral nutrients, including Ca^{2+}, in the shoots (Baxter et al., 2009). Tonoplast-localized Ca^{2+}/H^+ transporter CATION EXCHANGER1 (CAX1) and CAX3 transport Ca^{2+} from the cytosol to the vacuole of Arabidopsis (*Arabidopsis thaliana*) leaf mesophyll cells (Hirschi et al., 1996; Conn et al., 2011; Manohar et al., 2011; Kumar et al., 2015; Pittman and Hirschi, 2016). A *cax1cax3* loss-of-function double mutant exhibits leaf growth defects and early senescence in the leaves when grown in soil and increased sensitivity to high Ca^{2+} concentrations when grown on agar medium (Cheng et al., 2005). This mutant accumulates higher levels of Ca in the extracellular space than does Columbia-0 (Col-0), as revealed by x-ray analysis and field emission scanning electron microscopy-based mineral element microanalysis of cross sections of frozen-hydrated leaves (Conn et al., 2011).

The identity of the protein responsible for initial extracellular Ca^{2+} influx into the leaf cells after Ca^{2+} unloading from the xylem is unknown. In Arabidopsis, CNGC2 is predicted to be a cyclic nucleotide-gated channel and was initially identified as a key component of the hypersensitive response (HR), a rapid, local cell death response evoked by avirulent pathogens (Yu et al., 1998; Clough et al., 2000). The HR is an important self-protection mechanism whereby plants preserve whole leaves by undergoing localized cell death at the infection site. Although the *cngc2* mutant, which harbors a disruption in *CNGC2*, displays no localized cell death when grown in soil, its leaves maintain defense to avirulent pathogen infection (Yu et al., 1998; Clough et al., 2000). This observation has led to the notion that the HR is not necessary for plant cells to withstand infection by avirulent pathogens. Thus, the *cngc2* mutant also was named *defense no death* (*dnd1*; Yu et al., 1998). However, the soil-grown mutant displays a leaf growth inhibition phenotype, constitutively accumulates high levels of salicylic acid (SA) and reactive oxygen species (Yu et al., 1998; Clough et al., 2000; McDowell et al., 2013), and exhibits conditional early senescence symptoms, reduced Ca concentrations in the leaf (Clough et al., 2000), and altered Ca and magnesium (Mg) contents in the seeds (McDowell et al., 2013). Despite this, and similar to the *cax1cax3* double mutant, *cngc2* grows as well as the wild-type Col-0 on agar-based medium in sterile conditions, unless the Ca^{2+} concentration is increased to 10 mM (Chan et al., 2003). To date, no clear mechanism has been proposed to explain all of the phenotypes of the *cngc2* mutant. In this study, we show that all of the reported leaf phenotypes of soil-grown *cngc2* could be indirect effects of its sensitivity to the Ca^{2+} supply, suggesting that the primary function of CNGC2 is to mediate the influx of apoplastic Ca^{2+} into the leaf cells. In addition, we report a new in vivo method to monitor extracellular Ca^{2+} dynamics in the leaf.

RESULTS

CNGC2 Is Required for Plant Ca Nutrition But Not for Leaf Development and the HR

To test for a role of CNGC2 in Arabidopsis Ca nutrition, we used a hydroponic system to control the amount of Ca^{2+} available to the root (Fig. 1). Col-0 and *cngc2-1* plants were initially grown in medium containing 0.1 mM Ca^{2+} for 3 weeks and then transferred to medium containing 0.1, 1, 5, or 10 mM Ca^{2+} for 8 d. When grown in 0.1 mM Ca^{2+}, *cngc2-1* grew as well as Col-0 (Fig. 1A); however, when subjected to 1, 5, or 10 mM Ca^{2+}, the *cngc2-1* plants but not Col-0 showed [Ca^{2+}]-dependent growth inhibition and developed leaf senescence symptoms (Fig. 1, A and B). The root length (Supplemental Fig. S1A) and fresh weight (Supplemental Fig. S1B) were comparable between the mutant and Col-0 under these conditions. In addition, the Ca^{2+}-sensitive phenotype of *cngc2-1* could be complemented by expressing wild-type *CNGC2* driven by its native promoter (*COM*, which denotes complemented with *CNGC2*; Fig. 1C). Extending the treatment to 30 d strongly inhibited the stem elongation and inflorescence development of *cngc2* but not of the Col-0 or *COM* plants (Fig. 1D). These results demonstrated that CNGC2 has an essential role in Ca^{2+} nutrition.

The Arabidopsis genome contains 20 *CNGC* genes (Ward, 2001), 15 of which we tested for their involvement in the Ca^{2+} growth phenotype, using the corresponding T-DNA insertion mutants. Besides *cngc2*, the only mutant that showed a leaf growth inhibition phenotype when grown on 10 mM Ca^{2+} was *cngc4* (Supplemental Fig. S2). *CNGC4* is the closest homolog of *CNGC2* in the Arabidopsis genome, and soil-grown *cngc4* has the same leaf-growth inhibition phenotype as *cngc2* (Jurkowski et al., 2004). To further explore this result, we grew two *cngc2* and *cngc4* mutant alleles as well as the *cngc2cngc4* double mutant and found that all of them showed similar [Ca^{2+}]-sensitive symptoms as the *cngc2-1* mutants (Fig. 1E). These results further demonstrated the vital role of CNGC2 in Ca^{2+} nutrition.

Leaves of soil-grown *cngc2-1* plants have spontaneous lesions, occasional cell death spots, and constitutively elevated SA contents and expression of *PR1* (Yu et al., 1998; Clough et al., 2000; McDowell et al., 2013). In this study, under 0.1 mM Ca^{2+} conditions, the leaves of *cngc2-1* and Col-0 had similar low levels of staining for cell death (Fig. 2A) and H_2O_2 (Fig. 2B) as well as basal levels of SA (Fig. 2C) and *PR1* gene expression (Fig. 2D). Treatment with 10 mM Ca^{2+} for 8 d significantly increased cell death (Fig. 2A), H_2O_2 (Fig. 2B), and SA accumulation (Fig. 2C) as well as *PR1* gene expression (Fig. 2D) in the leaves of *cngc2-1* but not of Col-0 and the *COM* plants. These findings demonstrated that the Ca^{2+} sensitivity of *cngc2-1* accounts for the spontaneous high SA, H_2O_2 production, and cell death spots in *cngc2-1* leaves.

The *cngc2* is also named *dnd1*, since the mutant maintains defense to avirulent pathogens without displaying

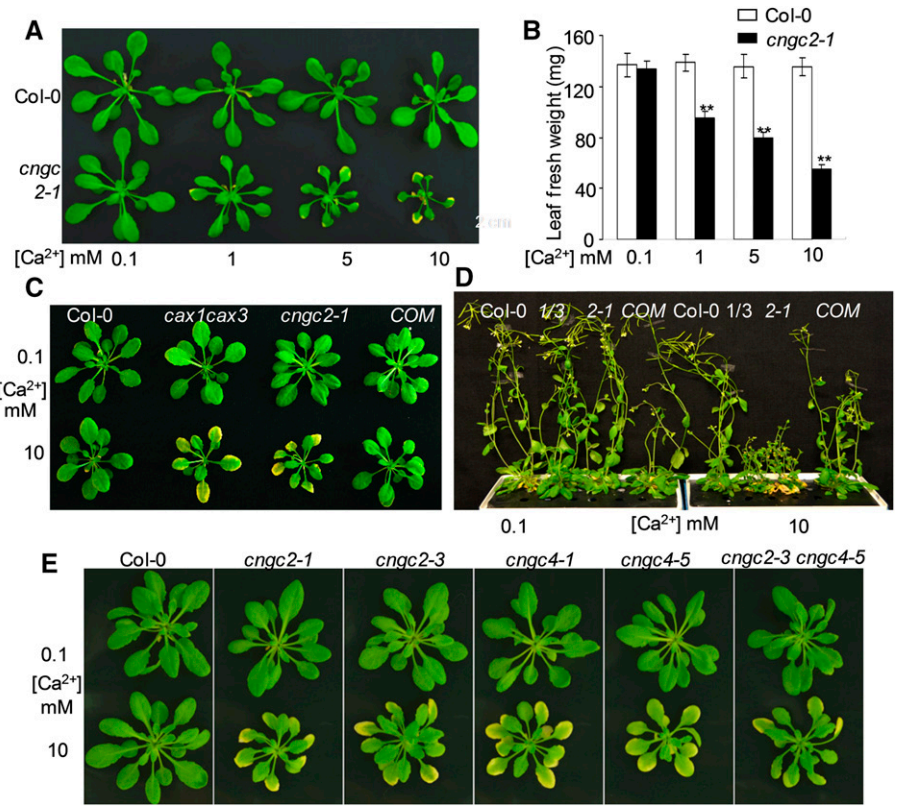

Figure 1. Arabidopsis hydroponics-grown *cngc2*, *cngc4*, and *cax1cax3* mutants are sensitive to the increasing [Ca^{2+}]. Arabidopsis plants were grown in hydroponic medium supplemented with 0.1 mM Ca^{2+} for 3 weeks and then transferred to medium containing the indicated concentrations of Ca^{2+}. A, Col-0 and *cngc2-1* were treated with 0.1, 1, 5, or 10 mM [Ca^{2+}] for 8 d. B, Leaf fresh weight of plants from A. Asterisks indicate significant differences between Col-0 and *cngc2-1*: **, $P < 0.01$. Values represent means ± SE; $n = 3$ biological trials with 40 plants per trial. C, Representative plants of Col-0, *cax1cax3*, *cngc2-1*, and *cngc2-1* complemented with *CNGC2* (*COM*) treated with 0.1 or 10 mM Ca^{2+} for 8 d. D, Representative plants of Col-0, *cax1cax3* (*1/3*), *cngc2-1* (*2-1*), and *COM* treated with 0.1 or 10 mM Ca^{2+} for 30 d. E, Representative plants of Col-0, *cngc2-3*, *cngc4-5*, and *cngc2-3cngc4-5* after 8 d of 10 mM Ca^{2+} treatment.

HR (Yu et al., 1998; Clough et al., 2000). To our knowledge, all of the reported *cngc2-1* (*dnd1*) HR phenotype characterizations were performed with leaves of soil-grown mutant plants showing early senescence or growth inhibition phenotypes (Yu et al., 1998; Clough et al., 2000; Ahn, 2007; Ali et al., 2007; Genger et al., 2008; Chin et al., 2013) similar to those in plants given 10 mM Ca^{2+} treatment using the hydroponics system in this study (Fig. 1). We reasoned that it was possible that the *dnd1* phenotype of *cngc2-1* is also Ca^{2+} supply dependent. To test this hypothesis, we infiltrated low (10^7 colony-forming units [cfu] mL^{-1}) and high (10^8 cfu mL^{-1}) densities of the avirulent pathogen *Pseudomonas syringae* pv *tomato* DC3000 expressing *avrRpm1* into leaves of Col-0, *cngc2-1*, *cngc2-3*, and *COM* plants. Under 0.1 mM Ca^{2+} growth conditions, all four genotypes displayed a typical HR (Fig. 3). A 3-d treatment with 10 mM Ca^{2+} did not cause obvious leaf senescence in the mutants and Col-0 but inhibited development of the HR in the leaves of *cngc2-1* but not of Col-0 and *COM*, in response to the low-density pathogen (Fig. 3). However, with the 10 mM Ca^{2+} treatment, all three genotypes displayed a normal HR in response to the high-density pathogen (10^8 cfu mL^{-1}; Fig. 3).

These data demonstrated that CNGC2 plays an essential role in plant Ca nutrition and that the previously observed leaf phenotypes of the soil-grown *cngc2* mutant could be an indirect result of CNGC2 function in Ca nutrition.

The *cngc2* Mutant and *cax1cax3* Double Mutants Have Similar Ca-Dependent Phenotypes

To dissect the underlying mechanism of CNGC2-mediated Ca nutrition, we measured total Ca contents in the leaves and roots of Col-0 and *cngc2-1* plants that we initially cultured on 0.1 mM Ca^{2+} and then treated for 3 d with 0.1, 1, or 10 mM Ca^{2+}. The 3-d treatments had no noticeable effects on the leaf growth and development of Col-0 and *cngc2-1*. Col-0 and *cngc2-1* had similar Ca contents in their leaves at 0.1 and 1 mM Ca^{2+}, and *cngc2-1* had significantly less Ca than Col-0 at 10 mM Ca^{2+} (Fig. 4A), which is similar to results with soil-grown plants (Clough et al., 2000; Ma et al., 2010). The total Ca content in *cngc2-1* roots was comparable to that of Col-0 (Fig. 4B). The Mg contents showed no difference between Col-0 and the mutant in both leaf and root (Fig. 4, C and D). These data imply that *cngc2-1* primarily was defective in Ca^{2+} distribution in the leaf but not in Ca^{2+} transport from the root to the leaf. This hypothesis was further supported by the observation that the detached leaves of *cngc2-1* developed similar senescence symptoms to those of intact plants under 10 mM [Ca^{2+}] (Fig. 4E). These findings suggested that *cngc2-1* was defective primarily in Ca^{2+} distribution in the leaf but not in Ca^{2+} transport from the root to the leaf.

The two most important genes known to be involved in Arabidopsis leaf Ca^{2+} nutrition are *CAX1* and *CAX3*, which encode Ca^{2+}/H^+ antiporters localized in the tonoplast of leaf mesophyll cells (Hirschi et al., 1996;

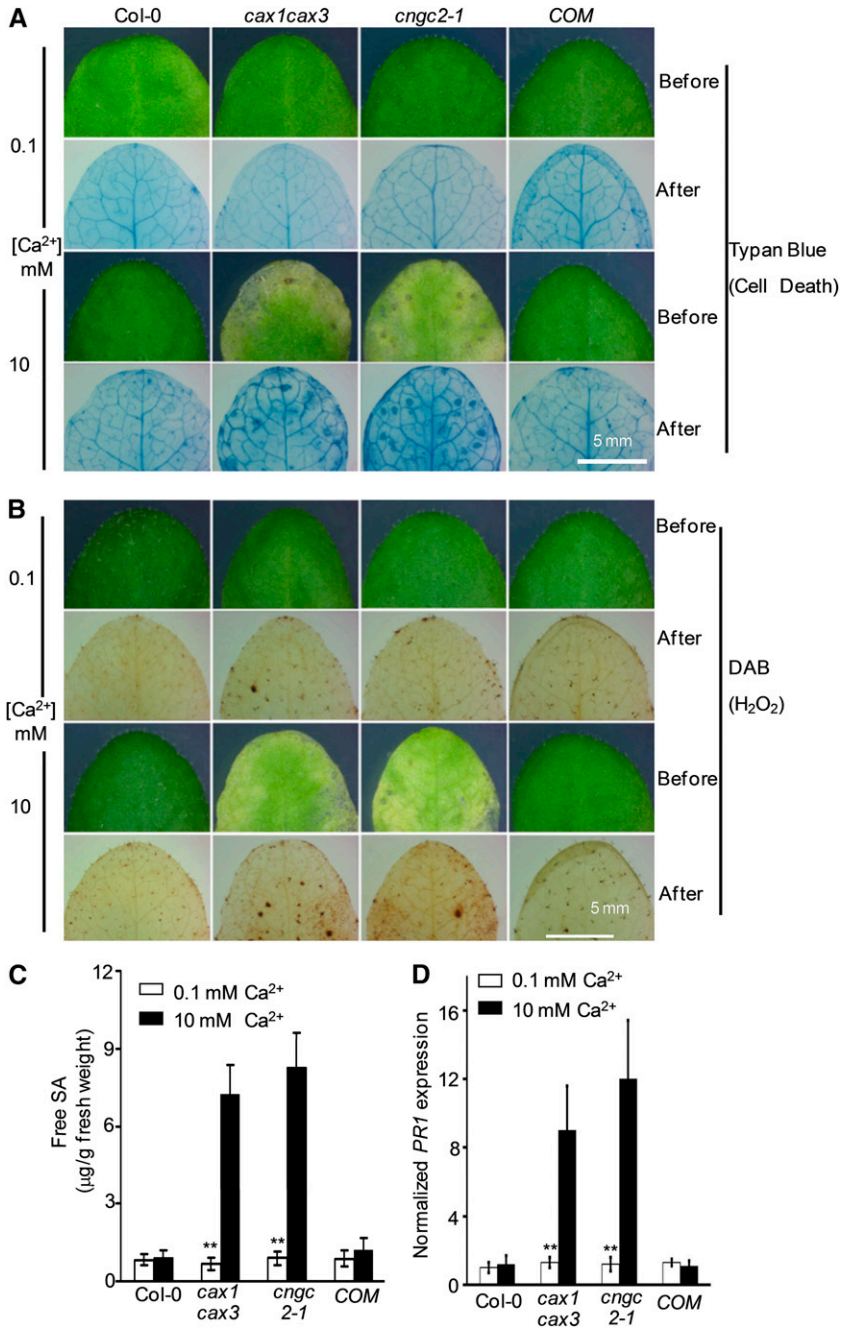

Figure 2. Increasing $[Ca^{2+}]$ promotes cell death and H_2O_2 and SA production in the leaves of *cax1cax3* and *cngc2* plants. A, Col-0, *cax1cax3*, *cngc2-1*, and *cngc2-1* complemented with *CNGC2* (*COM*) were initially grown on 0.1 mM Ca^{2+} and then treated with 0.1 or 10 mM Ca^{2+} for 8 d. Leaves with typical symptoms were examined with a dissecting microscope and stained with Trypan Blue for cell death, shown by dark blue spots. Images were taken before and after the staining. B, Plants were treated as in A and stained with 3,3-diaminobenzidine (DAB) for H_2O_2 accumulation, shown by brown spots. C, Free SA contents in the leaves of Col-0 and *cngc2-1* grown in the hydroponics system after 3 d of treatment with 0.1 or 10 mM Ca^{2+}. D, Plants were treated as in C, and *PR1* gene expression was examined and normalized to the internal standard and the *PR1* expression in Col-0 under 0.1 mM Ca^{2+} conditions. Values in C and D represent means ± SE; $n = 3$ biological trials. $^{**}P < 0.01$ between the 0.1 and 10 mM Ca^{2+} treatments.

Manohar et al., 2011; Kumar et al., 2015). The Arabidopsis *cax1cax3* double mutant has a very similar phenotype to that of *cngc2-1*: the soil-grown *cax1cax3* plants have growth defects and early senescence phenotypes; moreover, *cax1cax3* plants grown on agar-based medium are sensitive to 20 mM Ca^{2+} (Cheng et al., 2005). Disruption of *CAX1* and *CAX3* blocks cytosolic Ca^{2+} storage in the vacuole and causes Ca^{2+} to overaccumulate in the apoplast (Conn et al., 2011). By analogy, we wondered whether CNGC2 mediates Ca^{2+} influx into the mesophyll cells and if disrupting CNGC2 causes Ca^{2+} accumulation in the apoplast, which would account for the mutant's sensitivity to increasing Ca^{2+} supply to its roots. If CNGC2, CAX1, and CAX3 indeed function in same pathway mediating extracellular Ca^{2+} deposit to leaf cells, the *cax1cax3* and *cngc2* mutants might have similar Ca-dependent phenotypes. To test this hypothesis, we first grew Col-0, *cngc2-1*, *COM*, and *cax1cax3* plants on the agarose-based medium supplied with different $[Ca^{2+}]$ levels. Similar to *cngc2-1*, the growth of *cax1cax3* plants was no different compared with Col-0 at 0.1 mM Ca^{2+}, but its leaf growth (Supplemental Fig. S3, A and B) and root elongation (Supplemental Fig. S3C) were

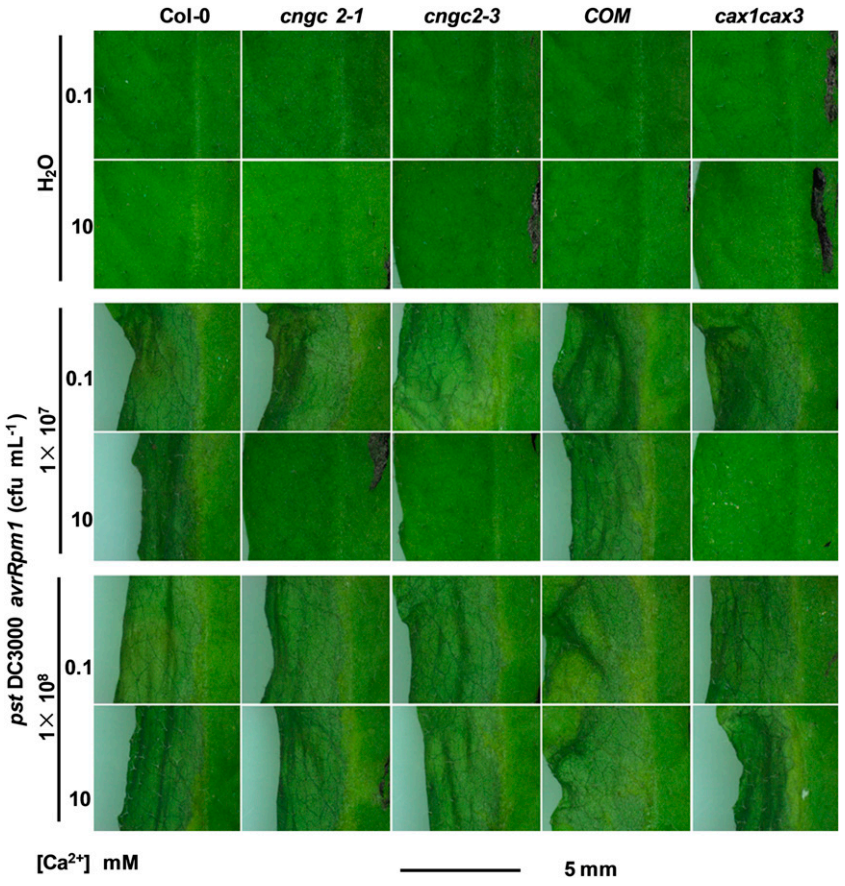

Figure 3. HR of Arabidopsis Col-0, *cngc2*, and *cax1cax3* mutants. Arabidopsis Col-0, *cngc2-1*, *cngc2-1* complemented with *CNGC2* (*COM*), and *cax1cax3* plants were first grown in hydroponic solution supplemented with 0.1 mM Ca^{2+} for 3 weeks and then subjected to 3-d treatments with 0.1 or 10 mM Ca^{2+}. The leaves were infiltrated with either water or a suspension of *P. syringae* pv *tomato* DC3000 *avrRpm1* in water at a density of 1×10^7 or 1×10^8 cfu mL^{-1}. Leaves with typical symptoms were photographed 24 h after infection.

suppressed significantly by increasing [Ca^{2+}]. In the hydroponic condition with 0.1 mM Ca^{2+}, the *cngc2-1* and *cax1cax3* mutants grew as well as Col-0 and *COM* (Fig. 1, C and D); however, the 8-d (Fig. 1C) or 30-d (Fig. 1D) 10 mM Ca^{2+} treatment inhibited *cax1cax3* leaf growth as much as that of *cngc2-1*, promoted senescence and cell death (Fig. 2A), induced the accumulation of H_2O_2 (Fig. 2B) and SA (Fig. 2C), and suppressed the HR induced by infection with avirulent pathogen at low density (Fig. 3). These results implied that CNGC2 and CAX1/CAX3 have similar functions in leaf Ca nutrition.

In Vivo Imaging of Extracellular Ca^{2+} in *cngc2* and *cax1cax3* Leaves

Disruption of the pathway from the cytosol to the vacuole for Ca^{2+} storage causes the apoplastic (extracellular) space of *cax1cax3* mutants to overaccumulate Ca, which was originally measured using x-ray microanalysis in fixed leaf cross sections (Conn et al., 2011). Although several luminescence- and fluorescence-based methods have been developed to measure intracellular Ca^{2+} distribution and dynamics in living plant cells (Knight et al., 1991; Behera et al., 2013), there has not been an in vivo method reported to date to visualize extracellular Ca^{2+} distribution in plant cells. In animal and human cells, Oregon Green BAPTA 488 5N (OGB-5N), a well-established membrane-impermeable low-affinity Ca^{2+} fluorescent dye (White and McGeown, 2002; Jiménez-Moreno et al., 2008), has been used to monitor extracellular Ca^{2+} dynamics (Rusakov and Fine, 2003), endocytosis-mediated extracellular Ca^{2+} uptake (Gerasimenko et al., 1998; Sherwood et al., 2007), and intracellular Ca^{2+} dynamics in giant cells like oocytes (Callamaras and Parker, 2000) and muscle cells (Hollingworth et al., 2009) through microinjection or the pipette during patch-clamp whole-cell recordings. Here, we developed a method to use OGB-5N in plants to track extracellular Ca^{2+} transport and distribution in the leaf.

We first grew Col-0 and *cngc2-1* in the hydroponic system with 0.1 mM Ca^{2+} and then applied a 3-d 0.1 or 10 mM Ca^{2+} treatment. Afterward, we placed the petioles of detached mature leaves from the hydroponics-cultured plants into the corresponding growth solutions containing OGB-5N. At time 0, no fluorescence was observed in all tested leaves (Fig. 5A). After 20 min, clear green fluorescence with similar patterns and intensity appeared in the vascular systems of Col-0 and *cngc2-1* in the 0.1 and 10 mM Ca^{2+} conditions (Fig. 5A). After 4 h of staining, leaves of both Col-0 and *cngc2-1* treated with 0.1 mM Ca^{2+} showed extracellular [Ca^{2+}] ($[Ca^{2+}]_{ext}$)-dependent green fluorescence primarily in the third

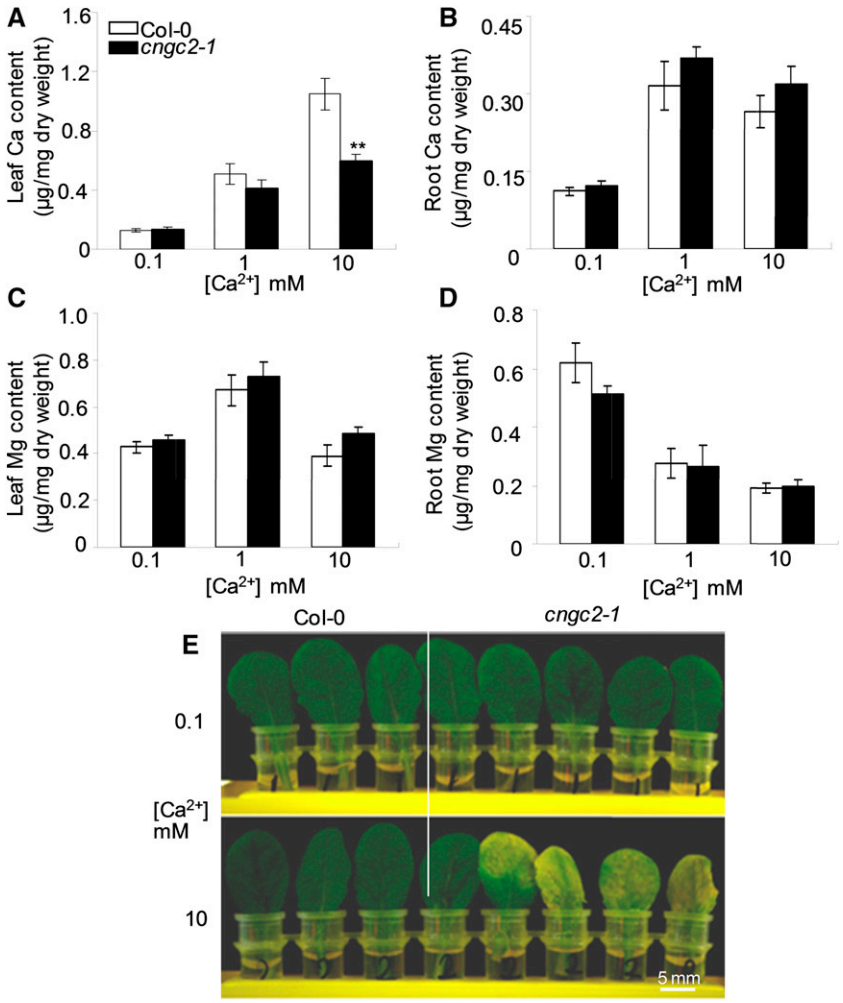

Figure 4. Ca and Mg contents of Col-0 and *cngc2-1* plants and their detached leaf responses to $[Ca^{2+}]$. A to D, Col-0 and *cngc2-1* initially were grown under hydroponic conditions with 0.1 mM Ca^{2+} for 3 weeks, then given 0.1, 1, or 10 mM Ca^{2+} for 3 d. Ca contents in the leaves (A) and roots (B), and Mg contents in the leaves (C) and roots (D), were measured. Values represent means of three biological replicates ± SE. **, Significant difference at $P < 0.01$ with Student's *t* test between Col-0 and *cngc2-1* under the same treatment. E, Col-0 and *cngc2-1* initially were grown under hydroponic conditions with 0.1 mM Ca^{2+} for 3 weeks. Fully expanded leaves were detached and inserted into a 200-μL tube with full nutrition medium containing either 0.1 or 10 mM Ca^{2+} for 8 d. Leaves with typical symptoms are shown.

and minor veins, with no obvious difference between genotypes in terms of pattern and intensity (Fig. 5A). No detectable fluorescence was present in the nonvascular tissues (e.g. veinlet, the leaf areas divided by the veins; Fig. 5A). Thus, it appears that Ca^{2+} unloaded from the vascular system was actively redistributed into other leaf cells and that very little free Ca^{2+} was extracellular. In the leaves treated with 10 mM Ca^{2+}, the $[Ca^{2+}]_{ext}$-dependent green fluorescence was still restricted to the vascular tissues in Col-0 but it spread to the nonvascular tissues (veinlet) in *cngc2-1* leaves (Fig. 5A). This difference implied that disrupting CNGC2 causes extracellular Ca^{2+} accumulation around the leaf cells. Furthermore, in a separate set of experiments, extracellular Ca^{2+} accumulation around the leaf cells was observed with two alleles of *cngc2* and *cax1cax3* and was rescued back to the Col-0 phenotype in the complementation line *COM* (Fig. 5B).

To visualize the extracellular Ca^{2+} distribution in the leaf with higher spatial resolution, we used confocal laser scanning microscopy. The cell wall boundaries of the leaf cells were defined using the red fluorescent dye propidium iodide. At 0.1 mM Ca^{2+}, extracellular Ca^{2+} was detected exclusively in the vascular system (veins), with very little if any green fluorescence detected in the surrounded leaf areas (veinlet) of Col-0, *cax1cax3*, *cngc2-1*, and *COM* plants (Fig. 6). At 10 mM Ca^{2+}, the $[Ca^{2+}]_{ext}$-dependent green fluorescence was still almost exclusively present in the vascular tissues (veins) of Col-0 and *COM*, especially the minor veins, with very limited signal in the nonvascular leaf areas (veinlet; Fig. 6). However, a significant amount of extracellular Ca^{2+}-dependent green fluorescence was detected around veinlet areas in *cngc2* and *cax1cax3* leaves (Fig. 6).

Ca in plants can be in a water-soluble ionic form or chelated by cell wall components and other acidic compounds like oxalate (Gilliham et al., 2011). It has been suggested that Ca^{2+} overaccumulation in the extracellular space of the *cax1cax3* leaf can increase Ca^{2+} deposition into the cell wall and decrease Ca^{2+} in the cytoplasm (Conn et al., 2011). To investigate this hypothesis, Ca in the leaves of Col-0, *cngc2-1*, and *cax1cax3* with 3 d of exposure to either 0.1 or 10 mM Ca^{2+} was sequentially extracted with water, acetic acid, and HCl to isolate water-soluble Ca^{2+}, the Ca^{2+} bound to the cell wall, and Ca^{2+} in complexes with acid compounds,

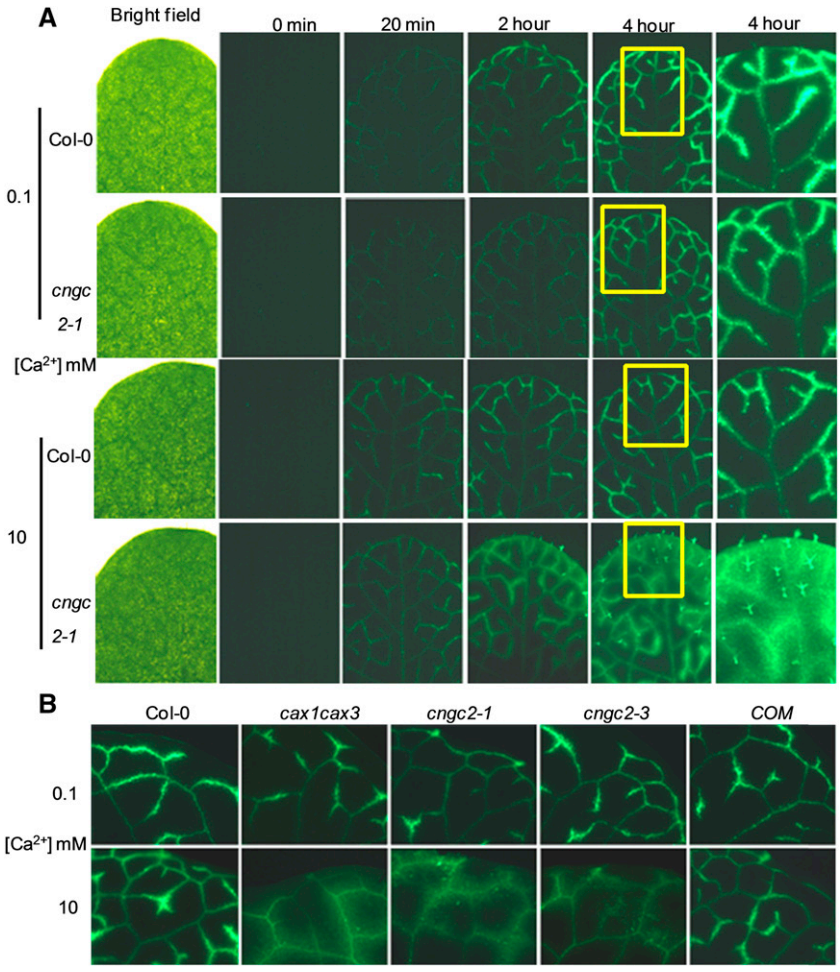

Figure 5. Fluorescence microscopy of extracellular Ca^{2+} in leaves of Col-0, *cngc2*, and *cax1cax3*. Col-0, *cngc2-1*, *cax1cax3*, and *cngc2-1* complemented with CNGC2 (*COM*) were hydroponically grown at 0.1 mM Ca^{2+} for 3 weeks and then given 3-d treatments of 0.1 or 10 mM Ca^{2+}. Fully expanded leaves were detached and inserted into 200-μL tubes with their corresponding growth medium in the presence of 20 μM Ca^{2+}-dependent fluorescent dye OGB-5N. A, Bright-field and fluorescence images of these leaves were taken at different time points of the OGB-5N treatment with either 2× or 10× objective lenses. The areas defined by the yellow squares in the 4-h (2×) images were magnified and are shown in the 4-h (10×) images. B, Treatment was the same as in A, and images were taken at 4 h.

respectively. After water and acetic acid extractions, we did not detect Ca in the HCl extract. With the 0.1 mM Ca^{2+} treatment, there was no significant difference between Col-0 and *cngc2-1* or *cax1cax3* in either water-soluble (Fig. 7, A and C) or acetic acid-soluble (Fig. 7, B and D) Ca^{2+} contents. However, at 10 mM Ca^{2+}, *cngc2-1* and *cax1cax3* plants had significantly less water-soluble Ca^{2+} (Fig. 7, A and C) but more acetic acid-soluble Ca^{2+} than Col-0 (Fig. 7, B and D). This result was consistent with the hypothesis that increasing the accumulation of Ca^{2+} in the extracellular space promotes Ca^{2+} deposition into the cell wall of *cngc2* and *cax1cax3* plants under high-Ca^{2+} growth conditions.

CNGC2 Is Expressed around Minor Veins and Encodes a Ca^{2+} Influx Channel

The Ca^{2+} overaccumulation in the extracellular space of *cngc2-1* leaf cells appeared preferentially in the areas surrounding the minor veins (Figs. 5 and 6), which might reflect cell-specific expression of *CNGC2*. For the 12-d-old seedlings grown on the agarose-based medium, *CNGC2* promoter activity was detected primarily in the leaves (Supplemental Fig. S4A) and weakly in the vascular tissue of the roots (Supplemental Fig. S4, B and C). For the mature plants grown on the hydroponics system, the *CNGC2* promoter activity was weakly detected in the stem (Supplemental Fig. S4D), flowers (Supplemental Fig. S4E), developing siliques (Supplemental Fig. S4F), and not in the roots (Supplemental Fig. S4G). In the leaf, besides the activity found in the cells surrounding trichomes (Supplemental Fig. S4H), *CNGC2* was expressed specifically in the vascular tissues and the leaf cells proximate to the vascular system, especially in the leaf areas around the free endings of minor veins, under both 0.1 and 10 mM Ca^{2+} conditions (Fig. 8A).

Free-ending areas of these minor veins are the primary places at which mineral ions, including Ca^{2+}, are unloaded from the vascular system and redistributed into the surrounding leaf cells (Ahn, 2007). Thus, it seemed that CNGC2 might function as a Ca^{2+} influx transporter mediating Ca^{2+} influx into the leaf cells immediately after Ca^{2+} unloading from the vascular tissues. Indirect evidence has suggested that CNGC2 is a Ca^{2+} influx channel: the plasma membrane of *cngc2* guard cells lacks the cAMP-activated Ca^{2+} influx current (Ali et al., 2007), and CNGC2 mediates a cAMP-induced

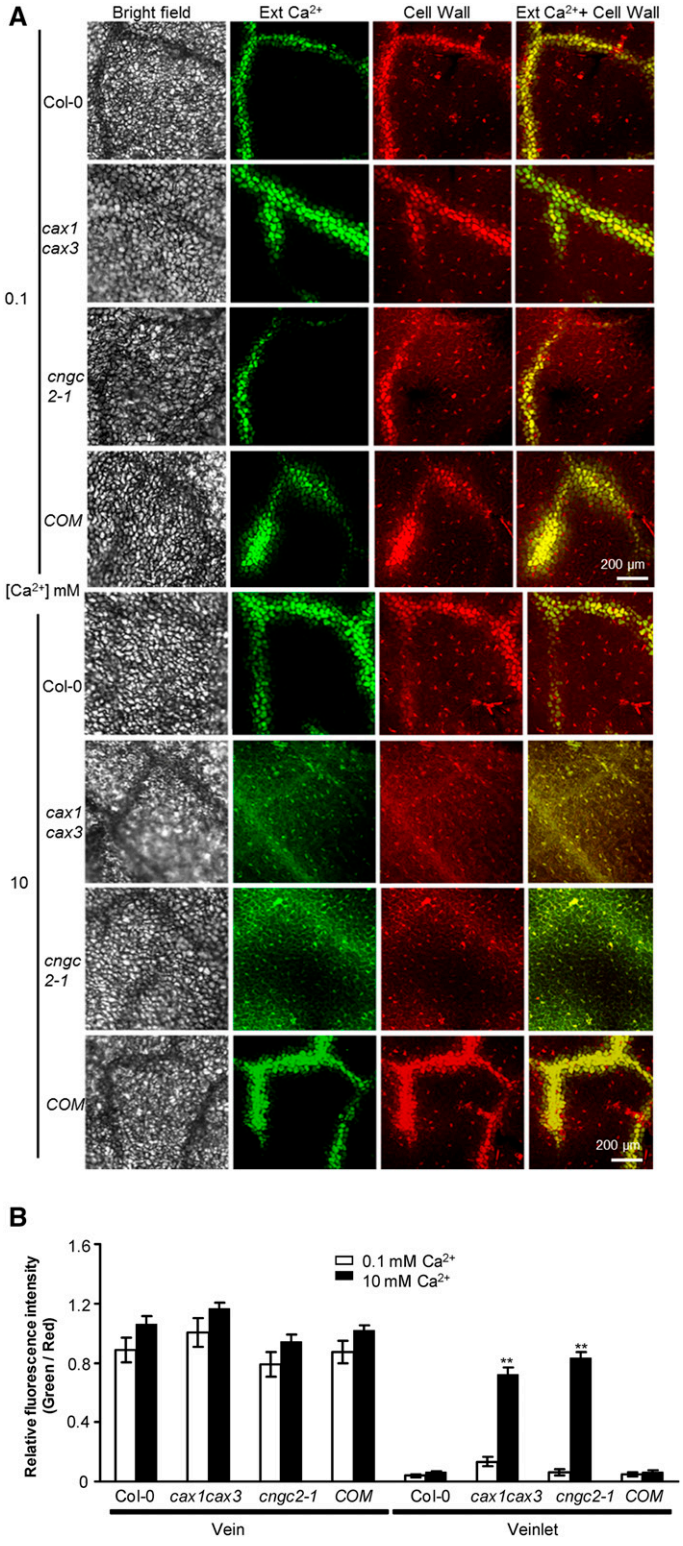

Figure 6. Confocal microscopy of extracellular Ca^{2+} in leaves of Col-0, *cngc2*, and *cax1cax3* plants. A, The plant growth and treatment procedures were the same as in Figure 7. The extracellular Ca^{2+} (Ext Ca^{2+}) and the cell wall boundary of the epidermal cells were visualized using the Ca^{2+}-dependent green fluorescent dye OGB-5N and red fluorescent dye propidium iodide, respectively, and observed by confocal laser scanning microscopy. Ext Ca^{2+} + Cell Wall indicates the merged images of Ext Ca^{2+} and Cell Wall. *COM* denotes the *cngc2-1* line complemented with *CNGC2*. B, Relative fluorescence intensity between the propidium iodide-dependent red and OGB-5N-dependent green signals was compared between Col-0 and mutants under 0.1 or 10 mM Ca^{2+} conditions in the vein and nonvein (veinlet) areas. Values represent means of three biological trials ± SE, with five leaves per trial and five areas per leaf. $^{**}P < 0.01$ between the 0.1 and 10 mM Ca^{2+} treatments.

increase in cytosolic Ca^{2+} when it is expressed in mammalian HEK293 cells (Leng et al., 1999). Recently, CNGC18, one of 20 CNGCs in Arabidopsis, was demonstrated to have Ca^{2+} influx channel activity when expressed in HEK293T cells, as measured by a patch-clamp whole-cell configuration (Gao et al., 2014, 2016) with an experimental setup similar to that used for previous recordings of the CRACM1 Ca^{2+} channel (Vig et al., 2006). To test directly for CNGC2 channel activity, we used the same protocol to express and study CNGC2 in HEK293T cells.

With 10 mM Ca^{2+} in the bath, an inward current was observed in HEK293T cells expressing CNGC2 but not in the cells with empty vector (Supplemental Fig. S5). The CNGC2-dependent current showed a moderate response to the membrane-permeable lipophilic cAMP analog 8-bromoadenosine cAMP (Supplemental Fig. S5). There are five significant ions in the recording solutions: Ca^{2+}, Na^{+}, Cs^{+}, Mg^{2+}, and Cl^{-} (Vig et al., 2006; Gao et al., 2014, 2016). At room temperature (23°C), with the assumption that only a single ion has the ability to cross the membrane, the theoretical equilibrium potentials for the individual ions are 140 mV (Ca^{2+}), 69 mV (Na^{+}), −63 mV (Cs^{+}), −13 mV (Mg^{2+}), and −48 mV (Cl^{-}). The measured reverse membrane potential for the CNGC2-dependent current was close to 0 mV (Supplemental Fig. S5), which was not close enough to any of the theoretical equilibrium potentials that the ionic composition of the current could be determined. However, additional observations suggested that the CNGC2-dependent current had a Ca^{2+} influx component. First, this was strongly inhibited by adding Gd^{3+}, an inward Ca^{2+} channel inhibitor, into the bath solution (Fig. 8, B and C). Second, the theoretical equilibrium potential for Ca^{2+}, with 175 nM free Ca^{2+} inside the cell, is predicted to increase from 140 to 154 mV when the bath [Ca^{2+}] is increased from 10 to 30 mM; experimentally, the reverse potential of the CNGC2-dependent current showed a similarly positive shift from 0 to around 17 mV (Fig. 8, B and C). In addition, the measured reverse membrane potential for the CNGC2-dependent current (Fig. 8, B and C) was similar to those reported for CNGC18 (Gao et al., 2014, 2016) and CRACM1 (Vig et al., 2006) Ca channels under the same ionic recording conditions. These data support the conclusion that CNGC2 has Ca^{2+} influx channel activity.

CNGC2 shows inward K^{+} channel activity when expressed in oocytes (Leng et al., 1999). By contrast, CNGC18 does not have inward K^{+} channel activity in

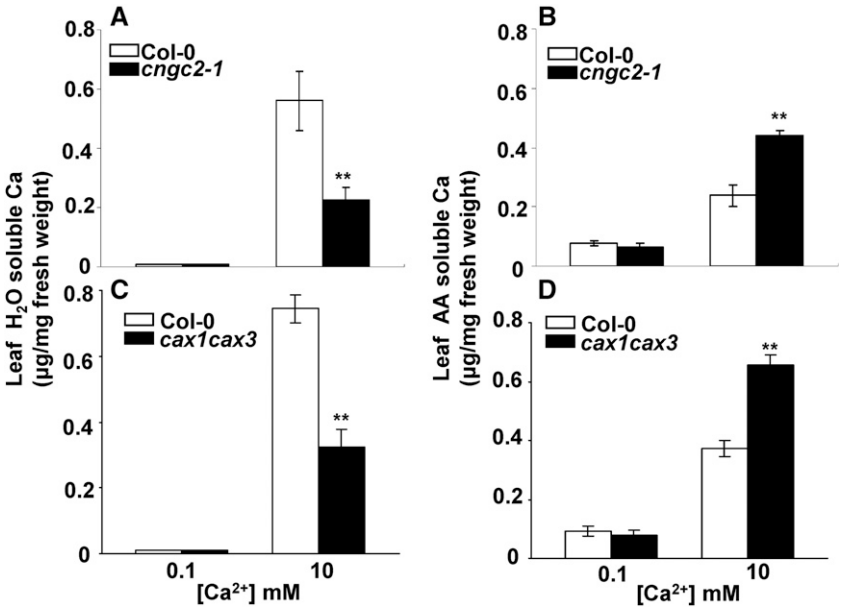

Figure 7. Water- and acetic acid-soluble Ca in the leaves of Col-0, *cngc2-1*, and *cax1cax3*. Col-0, *cngc2-1*, and *cax1cax3* plants were grown hydroponically with 0.1 mM Ca^{2+} for 3 weeks and then given a 3-d treatment with 0.1 or 10 mM Ca^{2+}. Fully expanded leaves were detached and extracted with water (A and C) for Ca content measurement. After the water extraction, the concentrated tissues were sequentially extracted with acetic acid (AA) for Ca content measurement (B and D). Values represent means ± SE; $n = 3$ biological trials, five replicates per trial, and leaves from four plants per replicate. **, $P < 0.01$.

HEK293T cells (Gao et al., 2014). Here, we did not detect inward K^+ channel activity in the CNGC2-expressing HEK293T cells (Supplemental Fig. S5), although the KAT1 positive control showed typical inward K^+ channel activity (Supplemental Fig. S6). In summary, we conclude that CNGC2, similar to CNGC18 (Gao

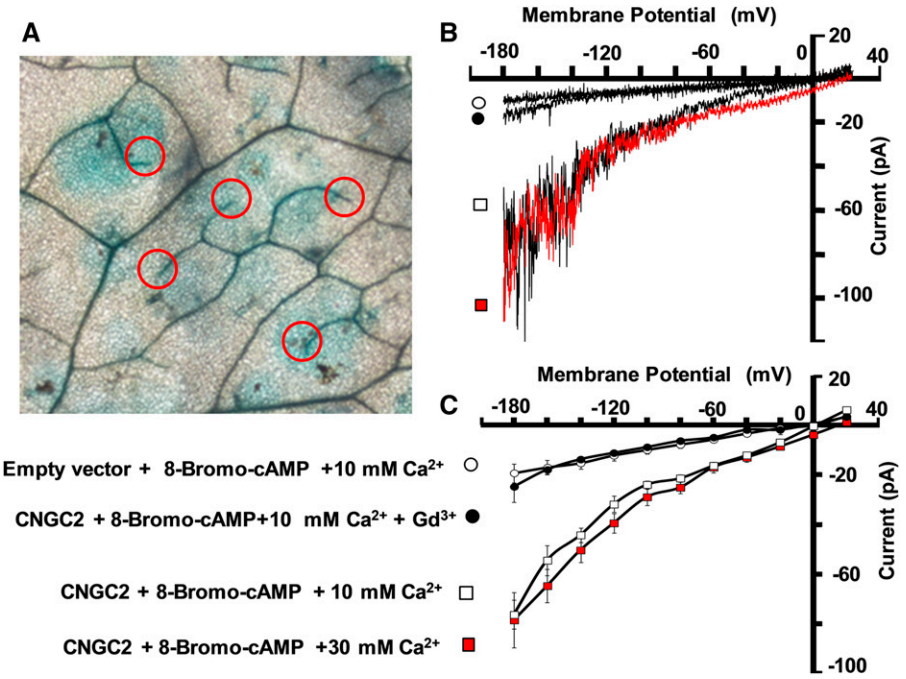

Figure 8. *CNGC2* minor vein area-specific expression and inward Ca^{2+} channel activity in HEK293T cells. A, *GUS* reporter gene-based *CNGC2* gene expression pattern (blue areas) in the leaf at 0.1 mM Ca^{2+}. The red circles indicate the positions of the minor vein free-ending areas. The pattern in the leaf at 10 mM Ca^{2+} was similar to that at 0.1 mM. B, *CNGC2* was transiently expressed in HEK293T cells. Patch-clamp whole-cell recording was used to monitor current across the plasma membrane under continuous voltage change from +20 to –180 mV. Representative recordings are shown under the indicated conditions. C, Average current-voltage curves are shown for the cell transformed with empty vector and recorded with 200 μM 8-bromoadenosine cAMP (8-Bromo-cAMP) and 10 mM Ca^{2+} in the bath solution ($n = 7$) and the cells transformed with *CNGC2* in bath solution containing 200 μM 8-Bromo-cAMP and 10 mM Ca^{2+} ($n = 6$), 10 mM Ca^{2+} + 1 mM $GdCl_3$ ($n = 5$), or 30 mM Ca^{2+} ($n = 9$). Values represent means ± SE.

et al., 2014), can mediate Ca^{2+} but not K^+ influx across the plasma membrane in HEK293T cells.

DISCUSSION

Plant growth and development depend on mineral nutrients absorbed by the roots and redistributed into leaves through the apoplast (extracellular space) and symplast (intracellular compartments) pathways, facilitated by transpiration and membrane-located mineral ion transporters, respectively (Kumar et al., 2015). Ca is an essential plant macronutrient with key roles in cellular signaling and structural integrity (Dodd et al., 2010; Kudla et al., 2010; Reddy et al., 2011; Yang et al., 2012). The physiological pathways mediating Ca absorption and distribution in plants are well studied (White and Broadley, 2003). However, the corresponding genetic mechanisms are largely unknown (Kudla et al., 2010; Spalding and Harper, 2011). In this study, we have provided several lines of evidence to support a key role of CNGC2 in mediating Ca^{2+} influx into Arabidopsis leaf cells after unloading from the vascular tissues (Fig. 9). First, CNGC2 shows Ca^{2+} influx channel activity when expressed in HEK293T cells (Fig. 8, B and C). Second, *CNGC2* is expressed predominantly in the leaf cells surrounding the free endings of the minor veins, which are the primary sites for Ca^{2+} unloading from the vascular tissues into the leaf cells (Fig. 8A). Third, disrupting *CNGC2* caused a significant amount of Ca^{2+} to accumulate in the extracellular space of leaf epidermal cells, similar to *cax1cax3* double mutants, which are known to be defective in Ca^{2+} transport from the extracellular space to the intracellular compartments (Figs. 5 and 6). Finally, at 0.1 mM Ca^{2+}, the *cngc2* mutant grew as well as the wild type; however, increasing the $[Ca^{2+}]$ induced cell death, H_2O_2 and SA accumulation (Fig. 2), as well as growth inhibition in the leaves of *cngc2-1* but not of the wild type (Fig. 1), which indicates the importance for plant cells to maintain low extracellular Ca^{2+} through CNGC2-mediated deposition of Ca^{2+} into leaf cells.

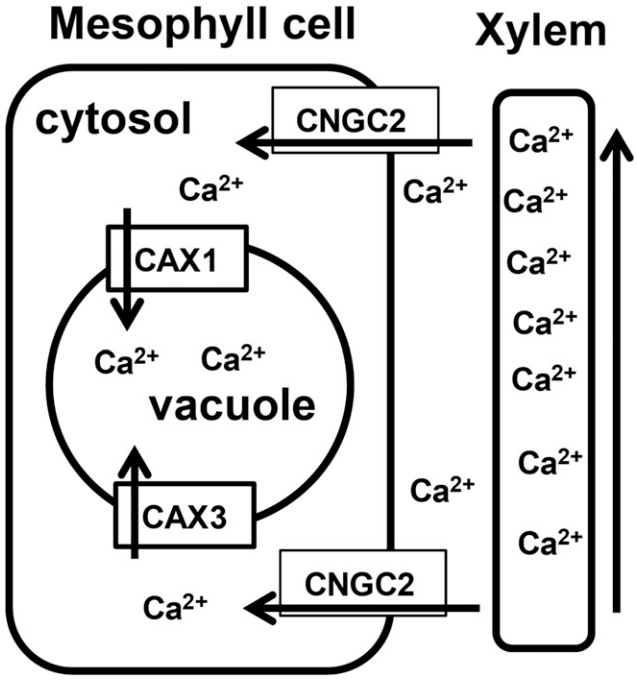

Figure 9. Model of CNGC2, CAX1, and CAX3 function in the transport of Ca^{2+} from the apoplast to the vacuole in Arabidopsis leaves. Ca^{2+} is absorbed by roots and transported upward to the apoplastic space of the leaf through the xylem driven by the leaf transpiration stream. After the Ca^{2+} in the xylem unloads into the apoplastic space of the leaf cells, it subsequently is transported into the cytosol through the plasma membrane-localized CNGC2 channel. The Ca^{2+} in the cytosol is sequestered into the vacuole via the tonoplast-localized Ca^{2+}/H^+ antiporters CAX1 and CAX3.

Since the discovery of the first CNGC2 loss-of-function mutant *dnd1* (*cngc2-1*) in 1998, it has been noted that the mutant leaves on soil-grown plants are smaller and senesce earlier than those of wild-type plants (Yu et al., 1998). In addition, the mutant leaves have constitutively higher accumulation of H_2O_2 and SA than the wild-type leaves when grown in soil (Yu et al., 1998; Clough et al., 2000). However, the mutant grows normally, like the wild type, when grown on agar medium in petri dishes unless the $[Ca^{2+}]$ increases to 10 mM (Chan et al., 2003). In this study, by controlling the Ca^{2+} supply to the roots through a hydroponic growth system (Fig. 1), we demonstrated that it was the increasing $[Ca^{2+}]_{ext}$ that was responsible for the observed leaf phenotypes of the mutant. It is possible that disrupting CNGC2 decreases the Ca^{2+} uptake capacity of the leaf cells near the minor veins. With low Ca^{2+} supply, the remaining Ca^{2+} uptake capacity of the *cngc2* leaf cells still would efficiently absorb the Ca^{2+} in the extracellular space that was unloaded from the vascular tissues, to maintain a low $[Ca^{2+}]_{ext}$. However, when the Ca^{2+} supply increased, the amount of Ca^{2+} absorbed by the mutant leaf cells would not be able to keep pace with the amount of Ca^{2+} unloading from the vascular tissue, which in turn would lead to Ca^{2+} overaccumulation in the extracellular space of the mutant cells (Fig. 9).

The data presented in this study demonstrate that maintaining a low $[Ca^{2+}]_{ext}$ is essential for the physiological functions of leaf cells and that CNGC2 plays a key role in this process. The increase of the $[Ca^{2+}]_{ext}$ due to the inactivation of CNGC2 interrupts multiple aspects of leaf function through largely unknown cellular and genetic pathways. Increasing $[Ca^{2+}]_{ext}$ activates class III peroxidase in the apoplast, which further promotes the degradation of H_2O_2 (Hepler and Winship, 2010). The plasma membrane-localized superoxide-generating NADPH oxidase RBOHD can be activated by the cytosolic $[Ca^{2+}]$ either directly or indirectly, which is responsible for the H_2O_2 burst in the apoplast (Hepler and Winship, 2010). In addition, H_2O_2 can activate a Ca^{2+}-permeable channel in the plasma membrane of the root and guard cells (Hepler and Winship, 2010). An increase in cytosolic $[Ca^{2+}]$ can activate SA biosynthesis through

Ca^{2+}-binding proteins (Seyfferth and Tsuda, 2014). However, it is unknown how the increase of $[Ca^{2+}]_{ext}$ is linked to H_2O_2 and SA production. Moreover, increases in $[Ca^{2+}]_{ext}$ can suppress water flow in leaf, which might interfere with photosynthesis (Gilliham et al., 2011).

It is well documented that the leaves of soil-grown *dnd1* (*cngc2-1*) mutants lack an HR but maintain their defenses against avirulent pathogen infection (Yu et al., 1998; Ali et al., 2007). In this study, the mutant leaf had a perfect HR when its root was supplied with 0.1 mM Ca^{2+} (Fig. 3). Three-day treatment with high $[Ca^{2+}]$ (10 mM) could suppress the HR induced by infection with the pathogen at low density but not at high density (Fig. 3). These data demonstrated that CNGC2 is not essential for the HR. The mutant's defective HR in response to the low-density avirulent pathogen in this study could be an indirect consequence of the overaccumulation of Ca^{2+} in the apoplast. We hypothesize that the increase of $[Ca^{2+}]_{ext}$ enhances the interaction of the Ca^{2+} with pectin and further strengthens the cell wall (Hepler and Winship, 2010), which could protect the leaf cell from death as a response to the avirulent pathogen (Choi et al., 2013; Mortimer et al., 2013; Johansson et al., 2014) but also could limit cell extensibility and decrease its growth rate. This possibility is supported by the findings that *cax1cax3* mutant leaf cell wall rigidity is increased under high $[Ca^{2+}]$ conditions (Conn et al., 2011).

In conclusion, this study not only identifies CNGC2 as the key factor mediating Ca^{2+} influx into the leaf cells after Ca^{2+} is unloaded into the apoplast from the vascular tissues but also provides an explanation for the growth and HR-defective phenotypes of the soil-grown *cngc2-1* (*dnd1*) mutant known since 1998 (Yu et al., 1998; Ali et al., 2007). Finally, the in vivo extracellular Ca^{2+} imaging method developed in this study provides a new tool for investigating Ca^{2+} dynamics in plant cells.

MATERIALS AND METHODS

Arabidopsis Growth Conditions and Pathogen Inoculation

To grow Arabidopsis (*Arabidopsis thaliana*) hydroponically, the seeds were sterilized with 75% and 100% ethanol for 15 and 5 min, respectively. The ethanol-treated seeds were dried on sterilized filter paper inside a hood. Twelve seeds were evenly distributed on an agarose-based control medium inside a petri dish, which contained the control solution with 0.1 mM $CaCl_2$ (Wang et al., 2015). After a 3-d treatment at 4°C, the petri dishes with seeds were put horizontally inside a growth chamber with 12/12-h light/dark period and 100 to 120 μmol m^{-2} s^{-1} light intensity. Three-week-old seedlings were transferred to a 5-mL tube hydroponics box containing the same nutrient solution as a control but without sugar and agar. The hydroponic solution was changed weekly. After another 3 weeks, the solution was changed to that with different concentrations of Ca^{2+} and other nutrients for the times indicated in the text. The *cngc2-1* (*dnd1*), *cngc2-3* (*salk_066908*), *cngc4-1* (*dnd2*), *cngc4-5* (*salk_081369*), and *cax1cax3* mutants were reported previously (Clough et al., 2000; Cheng et al., 2005; Genger et al., 2008; Liu et al., 2011; Chin et al., 2013). The *cngc2-3cngc4-5* double mutant was identified using PCR in the F2 population from F1 seeds created by cross-pollination of the two single mutants. Other *cngc* SALK mutants (Alonso et al., 2003) and primers used for homozygous identification are listed in Supplemental Table S1.

For the hypersensitive response assay, after 3-d treatments with either 0.1 or 10 mM Ca^{2+}, we infiltrated the avirulent pathogen *Pseudomonas syringae* pv *tomato* DC3000 *avrRpm* into the abaxial side of the leaves with a 1-mL syringe as described previously (Li et al., 2013).

Ca and Mg Content Measurement by Atomic Absorption Spectrometry

The leaf or root tissues for Ca and Mg content measurements in Figure 4 were harvested and dried in an oven at 105°C for 5 to 6 d. The dried tissues were weighed and ground to powder, which was further extracted with 1.5 m HCl for 2 d. The samples were centrifuged at 12,000g for 30 min, and the supernatants were used for Ca and Mg measurement with an atomic absorption spectrometer (TAS-990; Beijing Purkinje General).

For the sequential Ca extraction in Figure 7, the leaves were immediately frozen in liquid nitrogen after harvest and ground into fine powder for weighing (Borer et al., 2004, 2012). The powder was transferred into a 50-mL tube, and 20 mL of ultrapure water from the ELGA Option-Q ultrapure water system was added. The basal Ca content in the water was below 10 μm as measured with the Amplite Rhod Red fluorescence-based Ca quantification kit (Biolite). The powder-containing tube was shaken at 180 rpm, at room temperature, overnight and subsequently centrifuged at 8,000g for 30 min. The supernatant was saved as the water-soluble Ca for Ca measurement. The pellet was washed once with the ultrapure water and put into a 50°C oven overnight. The dried pellet was dissolved in 20 mL of acetic acid and shaken at 180 rpm, at room temperature, overnight. After centrifugation at 8,000*g* for 30 min, the supernatant was saved as the acetic acid-soluble Ca for Ca measurement. The pellet was subjected to further extraction with HCl.

Reactive Oxygen Species and Cell Death Assays in Arabidopsis Leaf

Arabidopsis leaf cell death was monitored with a Trypan Blue (Sigma-Aldrich) staining assay as described at http://commonweb.unifr.ch/biol/pub/mauchgroup/staining.html. The method for the 3,3-diaminobenzidine (Sigma-Aldrich)-based reactive oxygen species staining assay was as described previously (Zou et al., 2015).

SA Measurement and Real-Time Reverse Transcription-PCR

Arabidopsis plants were cultured in hydroponic conditions with 0.1 mM Ca^{2+} for 3 weeks and then given either 0.1 (as a control) or 10 mM Ca^{2+} treatment. Afterward, the well-expanded leaves were collected and ground into fine powder in liquid nitrogen, 50 to 100 mg of which was added into 1 mL of extraction buffer containing propanol:water:HCl (2:1:0.002, v/v/v) and 50 ng of ^{2}H-labeled SA as an internal standard. The mixture was rotated at 100 rpm at 4°C for 1 h, after which 1 mL of dichloromethane was added and the sample was rotated at 100 rpm and 4°C for another 1 h. The mixture was then centrifuged at 12,000*g* at 4°C for 30 min. The tissue debris was found between the two layers of liquid phases. Solution (200 μL) from the bottom phase was taken for total SA quantification as described previously (Pan et al., 2010).

For RNA extraction, the leaf tissue fine powder was extracted with the TransZol Plant kit (Transgen Biotech). cDNA was synthesized with TransScript All-in-One First Strand cDNA Synthesis Supermix for qPCR with One-Step gDNA Removal (Transgen Biotech) following the manufacturer's instructions. Primers for the internal standards *TUBULIN β-SUBUNIT* (At5g44340) and *PR1* (At2g14610) were reported previously (Ma et al., 2010). Quantitative real-time PCR was performed using a SYBR Premix Ex Taq II (TaKaRa) in a qTOWER 2.2 real-time PCR system (Analytik). The level of gene transcript accumulation was first normalized to the internal standard *TUBULIN β-SUBUNIT* (At5g44340) and expressed relative to the *PR1* gene value in Col-0 under the 0.1 mM Ca^{2+} condition.

GUS Reporter Gene-Based Promoter Activity Assay

A 2,186-bp DNA fragment was amplified from the genome region upstream of the *CNGC2* start codon with Col-0 genomic DNA as a template. The primers used were 5′-CTAGAAGCTTCTCCAAGCCAAGCCTGGTTAAAATCGG-3′ and 5′-ATTGGATCCGATTGAAATAGAGGAACCACCATGGGAG-3′, the underlined portions of which are restriction enzyme sites for *Hin*dIII and *Bam*HI, respectively. The amplified DNA fragment was integrated into the *Hin*dIII and *Bam*HI cloning sites upstream of the *GUS* reporter gene inside the binary vector pORE R1. *Agrobacterium tumefaciens* strain GV3101 harboring the 2,186-bp DNA fragment-containing pORE R1 vector (Coutu et al., 2007) was used to transform Arabidopsis (Clough and Bent, 1998). Transgenic Arabidopsis screening and GUS assays were as described previously (Zou et al., 2015).

HEK293T Cell Culture, Transfection, and Patch-Clamp Whole-Cell Recording

The *CNGC2* coding sequence was amplified with primers 5′-CGGAATTCATGCCCTCTCACCCCAACTTCAT-3′ and 5′-CCCCGGGTTATTCGAGATGATCATGCGGTCG-3′, the underlined portions of which are restriction enzyme sites for *Eco*RI and *Sma*I, respectively. The fragment was integrated into the *Eco*RI and *Sma*I sites of the pCI-neo vector. *HEK293T* cells were purchased from the Institute of Biotechnology and Cell Biology, Chinese Academy of Science. The procedures for HEK293T cell culture, transfection, and patch-clamp whole-cell recording were as described previously (Vig et al., 2006; Gao et al., 2014, 2016). For cAMP treatment, 200 μM 8-bromoadenosine cAMP (Sigma-Aldrich) was used. The theoretical equilibrium potentials were calculated with an online Nernst Potential Calculator at http://www.physiologyweb.com/calculators/nernst_potential_calculator.html.

Observation of Extracellular Ca^{2+} Distribution with Fluorescence and Confocal Microscopy

The low-affinity cell-impermeable Ca^{2+} fluorescent dye OGB-5N with excitation and emission at 494 and 521 nm, respectively, was purchased from Thermo Fisher Scientific (O-6812) and dissolved in DMSO to make a 5 mM stock stored at −20°C without exposure to light. For visualizing extracellular Ca^{2+} distribution, a fully expanded mature leaf was detached from a hydroponically grown Arabidopsis plant, and its petiole was put into a PCR tube containing 100 μL of growth solution including 20 μM OGB-5N and either 0.1 or 10 mM $CaCl_2$ for the indicated periods of time. Afterward, the leaf was stained with 20 μM propidium iodide for 10 min. Images presented in Figure 5 were acquired with a fluorescence microscope (Nikon Eclipse Ti). Images presented in Figure 6 were acquired with a confocal laser scanning microscope (Zeiss 710).

Accession Numbers

Sequence data for this article can be found in The Arabidopsis Information Resource at www.arabidopsis.org under the following accession numbers: AtCNGC2 (At5g15410), AtCNGC4 (At5g54250), AtCAX1 (At2g38170), and AtCAX3 (At3g51860).

Supplemental Data

The following supplemental materials are available.

Supplemental Figure S1. Root responses of *cngc2-1* to different Ca^{2+} concentrations in a hydroponic system.

Supplemental Figure S2. Responses of hydroponically grown Arabidopsis *cngc* mutants to Ca^{2+}.

Supplemental Figure S3. Ca-dependent growth of *cngc2-1* and *cax1cax3* seedlings.

Supplemental Figure S4. *CNGC2* promoter-driven *GUS* reporter gene expression in Arabidopsis young seedlings and mature plants.

Supplemental Figure S5. CNGC2 shows inward Ca^{2+} channel activity in HEK293T cells.

Supplemental Figure S6. Inward K^+ channel activity of CNGC2 and KAT1 in HEK293T cells.

Supplemental Table S1. Primer list for the identification of Arabidopsis *cngc* homozygous mutants.

ACKNOWLEDGMENTS

We thank Dr. Yong-Fei Wang at the Institute of Plant Physiology and Ecology, Chinese Academy of Sciences, for instruction on HEK293T cell-based patch-clamp experiments as well as Dr. Kendal D. Hirschi at Texas A&M University and Dr. Ying-Shin Chen at the Agricultural Biotechnology Research Center, Taiwan, for *cax1cax3* seeds.

Received August 4, 2016; accepted December 16, 2016; published December 20, 2016.

LITERATURE CITED

Ahn IP (2007) Disturbance of the Ca^{2+}/calmodulin-dependent signalling pathway is responsible for the resistance of Arabidopsis dnd1 against Pectobacterium carotovorum infection. Mol Plant Pathol **8:** 747–759

Ali R, Ma W, Lemtiri-Chlieh F, Tsaltas D, Leng Q, von Bodman S, Berkowitz GA (2007) Death don't have no mercy and neither does calcium: *Arabidopsis* CYCLIC NUCLEOTIDE GATED CHANNEL2 and innate immunity. Plant Cell **19:** 1081–1095

Alonso JM, Stepanova AN, Leisse TJ, Kim CJ, Chen H, Shinn P, Stevenson DK, Zimmerman J, Barajas P, Cheuk R, et al (2003) Genome-wide insertional mutagenesis of Arabidopsis thaliana. Science **301:** 653–657

Baker A, Ceasar SA, Palmer AJ, Paterson JB, Qi W, Muench SP, Baldwin SA (2015) Replace, reuse, recycle: improving the sustainable use of phosphorus by plants. J Exp Bot **66:** 3523–3540

Baxter I, Hosmani PS, Rus A, Lahner B, Borevitz JO, Muthukumar B, Mickelbart MV, Schreiber L, Franke RB, Salt DE (2009) Root suberin forms an extracellular barrier that affects water relations and mineral nutrition in Arabidopsis. PLoS Genet **5:** e1000492

Bedison JE, Johnson AH (2010) Seventy-four years of calcium loss from forest soils of the Adirondack Mountains, New York. Soil Sci Soc Am J **74:** 2187–2195

Behera S, Krebs M, Loro G, Schumacher K, Costa A, Kudla J (2013) Ca^{2+} imaging in plants using genetically encoded Yellow Cameleon Ca^{2+} indicators. Cold Spring Harb Protoc **2013:** 700–703

Borer CH, Hamby MN, Hutchinson LH (2012) Plant tolerance of a high calcium environment via foliar partitioning and sequestration. J Arid Environ **85:** 128–131

Borer CH, Schaberg PG, DeHayes DH, Hawley GJ (2004) Accretion, partitioning and sequestration of calcium and aluminum in red spruce foliage: implications for tree health. Tree Physiol **24:** 929–939

Callamaras N, Parker I (2000) Ca^{2+}-dependent activation of Cl^- currents in Xenopus oocytes is modulated by voltage. Am J Physiol Cell Physiol **278:** C667–C675

Chan CW, Schorrak LM, Smith RK Jr, Bent AF, Sussman MR (2003) A cyclic nucleotide-gated ion channel, CNGC2, is crucial for plant development and adaptation to calcium stress. Plant Physiol **132:** 728–731

Cheng NH, Pittman JK, Shigaki T, Lachmansingh J, LeClere S, Lahner B, Salt DE, Hirschi KD (2005) Functional association of Arabidopsis CAX1 and CAX3 is required for normal growth and ion homeostasis. Plant Physiol **138:** 2048–2060

Chin K, DeFalco TA, Moeder W, Yoshioka K (2013) The Arabidopsis cyclic nucleotide-gated ion channels AtCNGC2 and AtCNGC4 work in the same signaling pathway to regulate pathogen defense and floral transition. Plant Physiol **163:** 611–624

Choi HW, Kim NH, Lee YK, Hwang BK (2013) The pepper extracellular xyloglucan-specific endo-β-1,4-glucanase inhibitor protein gene, CaXEGIP1, is required for plant cell death and defense responses. Plant Physiol **161:** 384–396

Clough SJ, Bent AF (1998) Floral dip: a simplified method for Agrobacterium-mediated transformation of Arabidopsis thaliana. Plant J **16:** 735–743

Clough SJ, Fengler KA, Yu IC, Lippok B, Smith RK Jr, Bent AF (2000) The Arabidopsis dnd1 "defense, no death" gene encodes a mutated cyclic nucleotide-gated ion channel. Proc Natl Acad Sci USA **97:** 9323–9328

Conn SJ, Gilliham M, Athman A, Schreiber AW, Baumann U, Moller I, Cheng NH, Stancombe MA, Hirschi KD, Webb AA, et al (2011) Cell-specific vacuolar calcium storage mediated by CAX1 regulates apoplastic calcium concentration, gas exchange, and plant productivity in *Arabidopsis*. Plant Cell **23:** 240–257

Coutu C, Brandle J, Brown D, Brown K, Miki B, Simmonds J, Hegedus DD (2007) pORE: a modular binary vector series suited for both monocot and dicot plant transformation. Transgenic Res **16:** 771–781

Dodd AN, Kudla J, Sanders D (2010) The language of calcium signaling. Annu Rev Plant Biol **61:** 593–620

Gao QF, Fei CF, Dong JY, Gu LL, Wang YF (2014) Arabidopsis CNGC18 is a Ca^{2+}-permeable channel. Mol Plant **7:** 739–743

Gao QF, Gu LL, Wang HQ, Fei CF, Fang X, Hussain J, Sun SJ, Dong JY, Liu H, Wang YF (2016) Cyclic nucleotide-gated channel 18 is an essential Ca^{2+} channel in pollen tube tips for pollen tube guidance to ovules in Arabidopsis. Proc Natl Acad Sci USA **113:** 3096–3101

Genc Y, Tester M, McDonald GK (2010) Calcium requirement of wheat in saline and non-saline conditions. Plant Soil **327:** 331–345

Genger RK, Jurkowski GI, McDowell JM, Lu H, Jung HW, Greenberg JT, Bent AF (2008) Signaling pathways that regulate the enhanced disease resistance of Arabidopsis "defense, no death" mutants. Mol Plant Microbe Interact **21:** 1285–1296

Gerasimenko JV, Tepikin AV, Petersen OH, Gerasimenko OV (1998) Calcium uptake via endocytosis with rapid release from acidifying endosomes. Curr Biol **8:** 1335–1338

Gilliham M, Dayod M, Hocking BJ, Xu B, Conn SJ, Kaiser BN, Leigh RA, Tyerman SD (2011) Calcium delivery and storage in plant leaves: exploring the link with water flow. J Exp Bot **62:** 2233–2250

Halman J, Schaberg P, Hawley G, Hansen C (2011) Potential role of soil calcium in recovery of paper birch following ice storm injury in Vermont, USA. For Ecol Manage **261:** 1539–1545

Hepler PK, Winship LJ (2010) Calcium at the cell wall-cytoplast interface. J Integr Plant Biol **52:** 147–160

Hirschi KD, Zhen RG, Cunningham KW, Rea PA, Fink GR (1996) CAX1, an H^+/Ca^{2+} antiporter from Arabidopsis. Proc Natl Acad Sci USA **93:** 8782–8786

Hollingworth S, Gee KR, Baylor SM (2009) Low-affinity Ca^{2+} indicators compared in measurements of skeletal muscle Ca^{2+} transients. Biophys J **97:** 1864–1872

Hong-Bo S, Li-Ye C, Ming-An S (2008) Calcium as a versatile plant signal transducer under soil water stress. BioEssays **30:** 634–641

Jiménez-Moreno R, Wang ZM, Gerring RC, Delbono O (2008) Sarcoplasmic reticulum Ca^{2+} release declines in muscle fibers from aging mice. Biophys J **94:** 3178–3188

Johansson ON, Fantozzi E, Fahlberg P, Nilsson AK, Buhot N, Tör M, Andersson MX (2014) Role of the penetration-resistance genes PEN1, PEN2 and PEN3 in the hypersensitive response and race-specific resistance in Arabidopsis thaliana. Plant J **79:** 466–476

Johnson AH, Moyer A, Bedison JE, Richter SL, Willig SA (2008) Seven decades of calcium depletion in organic horizons of Adirondack forest soils. Soil Sci Soc Am J **72:** 1824–1830

Jurkowski GI, Smith RK Jr, Yu IC, Ham JH, Sharma SB, Klessig DF, Fengler KA, Bent AF (2004) Arabidopsis DND2, a second cyclic nucleotide-gated ion channel gene for which mutation causes the "defense, no death" phenotype. Mol Plant Microbe Interact **17:** 511–520

Karley AJ, White PJ (2009) Moving cationic minerals to edible tissues: potassium, magnesium, calcium. Curr Opin Plant Biol **12:** 291–298

Knight MR, Campbell AK, Smith SM, Trewavas AJ (1991) Transgenic plant aequorin reports the effects of touch and cold-shock and elicitors on cytoplasmic calcium. Nature **352:** 524–526

Krapp A (2015) Plant nitrogen assimilation and its regulation: a complex puzzle with missing pieces. Curr Opin Plant Biol **25:** 115–122

Kudla J, Batistic O, Hashimoto K (2010) Calcium signals: the lead currency of plant information processing. Plant Cell **22:** 541–563

Kumar A, Singh UM, Manohar M, Gaur VS (2015) Calcium transport from source to sink: understanding the mechanism(s) of acquisition, translocation, and accumulation for crop biofortification. Acta Physiol Plant **37:** 1722

Leng Q, Mercier RW, Yao W, Berkowitz GA (1999) Cloning and first functional characterization of a plant cyclic nucleotide-gated cation channel. Plant Physiol **121:** 753–761

Leys BA, Likens GE, Johnson CE, Craine JM, Lacroix B, McLauchlan KK (2016) Natural and anthropogenic drivers of calcium depletion in a northern forest during the last millennium. Proc Natl Acad Sci USA **113:** 6934–6938

Li F, Wang J, Ma C, Zhao Y, Wang Y, Hasi A, Qi Z (2013) Glutamate receptor-like channel3.3 is involved in mediating glutathione-triggered cytosolic calcium transients, transcriptional changes, and innate immunity responses in Arabidopsis. Plant Physiol **162:** 1497–1509

Liu TY, Aung K, Tseng CY, Chang TY, Chen YS, Chiou TJ (2011) Vacuolar Ca^{2+}/H^+ transport activity is required for systemic phosphate homeostasis involving shoot-to-root signaling in Arabidopsis. Plant Physiol **156:** 1176–1189

Liu YB, Pan XB, Li JS (2015) A 1961-2010 record of fertilizer use, pesticide application and cereal yields: a review. Agron Sustain Dev **35:** 83–93

Ma W, Smigel A, Walker RK, Moeder W, Yoshioka K, Berkowitz GA (2010) Leaf senescence signaling: the Ca^{2+}-conducting Arabidopsis cyclic nucleotide gated channel2 acts through nitric oxide to repress senescence programming. Plant Physiol **154:** 733–743

Manohar M, Shigaki T, Hirschi KD (2011) Plant cation/H^+ exchangers (CAXs): biological functions and genetic manipulations. Plant Biol (Stuttg) **13:** 561–569

McDowell SC, Akmakjian G, Sladek C, Mendoza-Cozatl D, Morrissey JB, Saini N, Mittler R, Baxter I, Salt DE, Ward JM, et al (2013) Elemental concentrations in the seed of mutants and natural variants of Arabidopsis thaliana grown under varying soil conditions. PLoS ONE **8:** e63014

Mortimer JC, Yu X, Albrecht S, Sicilia F, Huichalaf M, Ampuero D, Michaelson LV, Murphy AM, Matsunaga T, Kurz S, et al (2013) Abnormal glycosphingolipid mannosylation triggers salicylic acid-mediated responses in *Arabidopsis*. Plant Cell **25:** 1881–1894

Närhi P, Middleton M, Gustavsson N, Hyvönen E, Sutinen ML, Sutinen R (2011) Importance of soil calcium for composition of understory vegetation in boreal forests of Finnish Lapland. Biogeochemistry **102:** 239–249

Pan X, Welti R, Wang X (2010) Quantitative analysis of major plant hormones in crude plant extracts by high-performance liquid chromatography-mass spectrometry. Nat Protoc **5:** 986–992

Pilbeam DJ (2015) Breeding crops for improved mineral nutrition under climate change conditions. J Exp Bot **66:** 3511–3521

Pittman JK, Hirschi KD (2016) CAX-ing a wide net: cation/H^+ transporters in metal remediation and abiotic stress signalling. Plant Biol (Stuttg) **18:** 741–749

Reddy AS, Ali GS, Celesnik H, Day IS (2011) Coping with stresses: roles of calcium- and calcium/calmodulin-regulated gene expression. Plant Cell **23:** 2010–2032

Robertson D (2013) Modulating plant calcium for better nutrition and stress tolerance. ISRN Botany **2013:** 952043

Rusakov DA, Fine A (2003) Extracellular Ca^{2+} depletion contributes to fast activity-dependent modulation of synaptic transmission in the brain. Neuron **37:** 287–297

Seyfferth C, Tsuda K (2014) Salicylic acid signal transduction: the initiation of biosynthesis, perception and transcriptional reprogramming. Front Plant Sci **5:** 697

Sherwood MW, Prior IA, Voronina SG, Barrow SL, Woodsmith JD, Gerasimenko OV, Petersen OH, Tepikin AV (2007) Activation of trypsinogen in large endocytic vacuoles of pancreatic acinar cells. Proc Natl Acad Sci USA **104:** 5674–5679

Spalding EP, Harper JF (2011) The ins and outs of cellular Ca^{2+} transport. Curr Opin Plant Biol **14:** 715–720

Talhelm AF, Pregitzer KS, Burton AJ, Zak DR (2012) Air pollution and the changing biogeochemistry of northern forests. Front Ecol Environ **10:** 181–185

Vig M, Peinelt C, Beck A, Koomoa DL, Rabah D, Koblan-Huberson M, Kraft S, Turner H, Fleig A, Penner R, et al (2006) CRACM1 is a plasma membrane protein essential for store-operated Ca^{2+} entry. Science **312:** 1220–1223

Wang J, Wang Y, Yang J, Ma C, Zhang Y, Ge T, Qi Z, Kang Y (2015) Arabidopsis ROOT HAIR DEFECTIVE3 is involved in nitrogen starvation-induced anthocyanin accumulation. J Integr Plant Biol **57:** 708–721

Wang Y, Wu WH (2015) Genetic approaches for improvement of the crop potassium acquisition and utilization efficiency. Curr Opin Plant Biol **25:** 46–52

Ward JM (2001) Identification of novel families of membrane proteins from the model plant Arabidopsis thaliana. Bioinformatics **17:** 560–563

White C, McGeown G (2002) Imaging of changes in sarcoplasmic reticulum $[Ca^{2+}]$ using Oregon Green BAPTA 5N and confocal laser scanning microscopy. Cell Calcium **31:** 151–159

White PJ (2001) The pathways of calcium movement to the xylem. J Exp Bot **52:** 891–899

White PJ, Broadley MR (2003) Calcium in plants. Ann Bot (Lond) **92:** 487–511

Yang J, Punshon T, Guerinot ML, Hirschi KD (2012) Plant calcium content: ready to remodel. Nutrients **4:** 1120–1136

Yu IC, Parker J, Bent AF (1998) Gene-for-gene disease resistance without the hypersensitive response in Arabidopsis dnd1 mutant. Proc Natl Acad Sci USA **95:** 7819–7824

Zou JJ, Li XD, Ratnasekera D, Wang C, Liu WX, Song LF, Zhang WZ, Wu WH (2015) *Arabidopsis* CALCIUM-DEPENDENT PROTEIN KINASE8 and CATALASE3 function in abscisic acid-mediated signaling and H_2O_2 homeostasis in stomatal guard cells under drought stress. Plant Cell **27:** 1445–1460